Modal contributions to the acoustic responses of fluid-loaded shells

Yegao Qu[1]; Hongxing Hua[1]; Herwig Peters[2]; Nicole Kessissoglou[2]

[1] School of Mechanical Engineering, Shanghai Jiao Tong University, Shanghai, China

[2] School of Mechanical and Manufacturing Engineering, UNSW Australia, Sydney, Australia

ABSTRACT

This work compares results from analytical and numerical techniques to predict the modal contributions to the radiated sound power and far-field sound pressure for structures submerged in a heavy fluid medium. A fluid-loaded cylindrical shell with hemispherical end caps is examined. The cylinder is excited by either axial or transverse forces acting at one end, to predominantly excite the lowest order cylinder circumferential modes. A modified variational method combined with a spectral boundary element method is used to develop an analytical model of the coupled hemispherical and cylindrical shells under heavy fluid loading conditions. The displacement components and the sound pressure are expanded in the form of a double mixed series using Fourier series and Chebyshev orthogonal polynomials. A fully coupled finite element/boundary element model of the same coupled hemispherical-cylindrical shell is also developed. A numerical technique for modal decomposition of the acoustic responses of the structure using the fluid-loaded structural modes is implemented. The individual contributions of the cylinder circumferential modes to the sound power and directivity of the radiated sound pressure are observed. The techniques presented here provide greater physical insight into structure-borne radiated noise from fluid-loaded shells.

Keywords: Radiated sound power, cylindrical shell, fluid loading I-INCE Classification of Subjects Number(s): 54.3

1. INTRODUCTION

Predicting the vibro-acoustic responses of thin shell structures in contact with an unbounded fluid is important in various engineering applications including underwater vehicles and submarines. Low frequency vibration modes of a thin shell can be easily excited by external forces, which may result in a high level of radiated noise. Identifying the modal contributions to the sound radiation of shell structures is useful to reduce the noise by refining the design of the structure. For an elastic shell in air, the structural and acoustic responses can be subsequently solved. However, for the case of a shell immersed in water where the fluid impedance is comparable to that of the shell, the fluid-structure interaction is strongly coupled and the structural and acoustic responses have to be simultaneously solved.

Prediction of the structure-borne radiated noise from fluid-loaded shells is a well defined fluid-structure interaction problem. A large amount of work has been devoted to this subject in the past few decades, for example, see Refs. (1-3). In general, analytical approaches for fluid-structure interaction problems are restricted to spherical shells and infinite cylindrical geometries using the classical method of separation of variables. For an arbitrarily shaped shell of revolution submerged in an unbounded fluid and subject to external forces of arbitrary type, numerical methods are preferable to analytical approaches. The coupled finite element method/boundary element method is a very powerful and popular tool for computing the vibro-acoustic responses of fluid-loaded structures (4-8). The finite element method is generally employed to describe the dynamic behavior of the structure whereas the boundary element method is used to represent the fluid domain and predict the acoustic responses.

The work examines the acoustic responses of a submerged vessel immersed in a heavy fluid of

[1] quyegao@sjtu.edu.cn (Y. Qu)
[2] herwig.peters@unsw.edu.au (H. Peters)

infinite extent. The vessel is simplified as a coupled shell consisting of a closed cylindrical shell with two hemispherical end caps. Since the geometrical configuration of the coupled shell is complex, analytical solutions for the fluid-structure interaction problem of the shell are not possible. A modified variational method in conjunction with a multi-segment partitioning technique is employed to formulate the structural model. A spectral Helmholtz integral equation is used to model the exterior fluid. The displacement components and radiated sound pressure are expanded in the form of a double mixed series using Fourier series and Chebyshev orthogonal polynomials. A finite element/boundary element model of the same coupled shell is also developed, in which the structural and fluid domain models are fully coupled using the mortar method. Modal decomposition of the acoustic responses of the structure using the fluid-loaded structural modes is implemented. Analytical and numerical results for the coupled shell subject to different excitation loads are presented. The individual contributions of the circumferential modes to the sound power and directivity of the radiated sound pressure are examined.

2. THEORTICAL FORMULATIONS

2.1 Model Description

Consider a cylindrical shell closed by two hemispherical end caps, as shown in Fig. 1. The hemispherical caps are described by spherical coordinates (φ, θ). The displacement components of the hemispherical shell in the φ, θ and normal directions are denoted by u_s, v_s and w_s, respectively. For the cylindrical shell, the middle surface is defined by the cylindrical coordinates (x, θ). The displacements related to the x, θ and normal directions are given by u_c, v_c and w_c, respectively. The coupled shell is made from an isotropic, homogeneous and linearly elastic material with Young's modulus E, Poisson's ratio μ and density ρ. The coupled shell structure is submerged in an unbounded heavy fluid. A global cylindrical coordinate system (r, θ, z) located at the geometrical centre of the coupled shell is introduced to describe the acoustic field. All pressures, displacements and velocities are presented by their complex, frequency dependent Fourier components with time dependence $e^{i\omega t}$, where ω is the angular frequency.

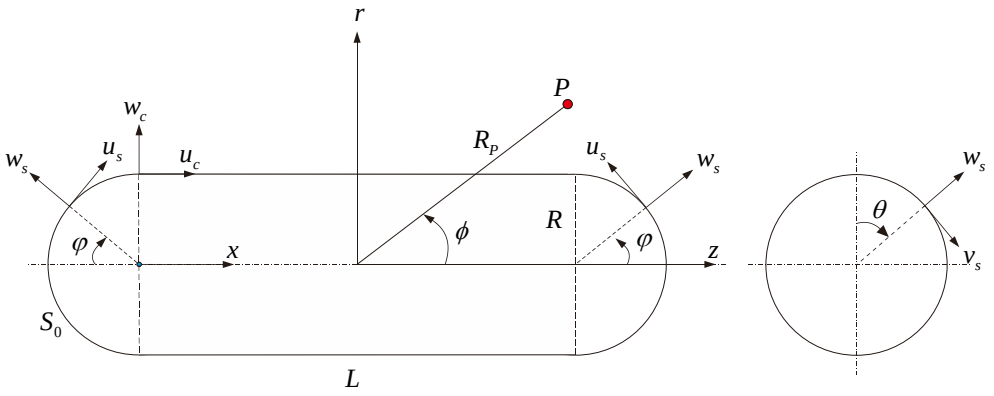

Figure 1 – Geometrical model and coordinate systems of the coupled cylindrical and hemispherical shells

2.2 Semi-analytical Model

Reissner's thin shell theory in conjunction with the modified variational method proposed by the first author and co-workers (9) is employed to formulate the structural model of the coupled shell. The structure is preliminary divided into cylindrical and hemispherical shell components at the junctions. The cylindrical shell component is further decomposed into N_c cylindrical shell segments in the x-direction. Similarly, each spherical shell is divided into N_s segments along the coordinate φ. The modified variational principle requires all displacements to satisfy the interface continuity conditions and the prescribed initial conditions at times $t = t_0$ and $t = t_1$ as follows

$$\int_{t_0}^{t_1} \sum_{m=1}^{N} \left(\delta T_m - \delta U_m + \delta W_m^s + \delta W_m^f \right) dt + \int_{t_0}^{t_1} \sum_{m,m'} \delta \Pi_{m,m'} dt = 0 \tag{1}$$

where N is the total number of shell segments, given as $N = N_c + 2N_s$. T_m and U_m are the kinetic and strain energies of the m^{th} shell segment, respectively. δ is a variational operator. δW_m^s denotes the virtual work done by mechanical forces that drive the coupled shell and δW_m^f represents the virtual work corresponding to the acoustic loading of the fluid external to the shell. $\Pi_{m,m'}$ is the interface potential on the common boundary of adjacent shell segments m and m', which is used to enforce interface continuity conditions on common boundaries. A detailed expression for $\Pi_{m,m'}$ can be found in Ref. (9).

The kinetic and stain energies of the m^{th} shell segment are given as

$$T_m = \frac{1}{2}\iint_{S_m} \rho h\left(\dot{u}_{\vartheta,m}^2 + \dot{v}_{\vartheta,m}^2 + \dot{w}_{\vartheta,m}^2\right) dS\,, \quad \vartheta = s,\ c \tag{2}$$

$$\begin{aligned} U_m = {} & \frac{K}{2}\iint_{S_m}\left\{(\varepsilon_\alpha^0)^2 + (\varepsilon_\theta^0)^2 + 2\mu\varepsilon_\alpha^0\varepsilon_\theta^0 + \frac{1-\mu}{2}(\varepsilon_{\alpha\theta}^0)^2\right\} dS \\ & + \frac{D}{2}\iint_{S_m}\left\{(\chi_\alpha^0)^2 + (\chi_\theta^0)^2 + 2\mu\chi_\alpha^0\chi_\theta^0 + \frac{1-\mu}{2}(\chi_{\alpha\theta}^0)^2\right\} dS \end{aligned}, \quad \alpha = x,\ \varphi \tag{3}$$

K and D are respectively the extensional and flexural rigidities, defined as $K = Eh/(1-\mu^2)$ and $D = Eh^3/[12(1-\mu^2)]$, where h is the thickness of the shell. S_m is the area of the m^{th} shell segment. ε_α^0, ε_θ^0 and $\varepsilon_{\alpha\theta}^0$ are the membrane strains of the reference surface. χ_α^0, χ_θ^0 and $\chi_{\alpha\theta}^0$ denote the curvature changes of the shell segment. Detailed expressions for the strain components and curvature changes of cylindrical and spherical shells are also found in Ref. (9).

The virtual work done by the mechanical forces is given by

$$\delta W_m^s = \iint_{S_m}\left(\delta u_{\vartheta,m} f_{u,m} + \delta v_{\vartheta,m} f_{v,m} + \delta w_{\vartheta,m} f_{w,m}\right) dS \tag{4}$$

where $f_{u,m}$, $f_{v,m}$ and $f_{w,m}$ are the mechanical forces acting on the coupled shell in the meridional, circumferential and normal directions, respectively. The virtual work done by the sound pressure of the external fluid is given by

$$\delta W_m^f = -\iint_{S_m} \delta w_{\vartheta,m} p_m dS \tag{5}$$

where p_m is the sound pressure acting on the m^{th} shell segment.

The displacement components of each shell segment are expanded by means of a double series. A Fourier series is used for the circumferential variable and orthogonal polynomials for the meridional variable. As a result, a two-dimensional problem is transformed into a set of uncoupled one-dimensional problems, which correspond to the harmonics of the Fourier expansion. For the m^{th} shell segment, the displacement components are expanded as follows

$$u_{\vartheta,m}(\alpha,\theta,t) = \sum_{q=0}^{Q}\sum_{n=0}^{\bar{N}} T_q(\alpha)\left[\cos(n\theta)\tilde{u}_{n,m}^q + \sin(n\theta)\bar{u}_{n,m}^q\right]e^{i\omega t} = \mathbf{U}_{\vartheta,m}(\alpha,\theta)\mathbf{u}_{\vartheta,m}e^{i\omega t} \tag{6a}$$

$$v_{\vartheta,m}(\alpha,\theta,t) = \sum_{q=0}^{Q}\sum_{n=0}^{\bar{N}} T_q(\alpha)\left[\sin(n\theta)\tilde{v}_{n,m}^q + \cos(n\theta)\bar{v}_{n,m}^q\right]e^{i\omega t} = \mathbf{V}_{\vartheta,m}(\alpha,\theta)\mathbf{v}_{\vartheta,m}e^{i\omega t} \tag{6b}$$

$$w_{\vartheta,m}(\alpha,\theta,t) = \sum_{q=0}^{Q}\sum_{n=0}^{\bar{N}} T_q(\alpha)\left[\cos(n\theta)\tilde{w}_{n,m}^q + \sin(n\theta)\bar{w}_{n,m}^q\right]e^{i\omega t} = \mathbf{W}_{\vartheta,m}(\alpha,\theta)\mathbf{w}_{\vartheta,m}e^{i\omega t} \tag{6c}$$

$T_q(\alpha)$ is the q^{th} order Chebyshev orthogonal polynomials of the first kind. Non-negative integer n represents the circumferential mode number. Q and $\bar{N}$ are respectively the highest degrees taken in the Chebyshev polynomials and Fourier series. $\tilde{u}_{n,m}^q$, $\tilde{v}_{n,m}^q$, $\tilde{w}_{n,m}^q$, $\bar{u}_{n,m}^q$, $\bar{v}_{n,m}^q$ and $\bar{w}_{n,m}^q$ are the generalized coordinate variables. $\mathbf{U}_{\vartheta,m}$, $\mathbf{V}_{\vartheta,m}$ and $\mathbf{W}_{\vartheta,m}$ denote the polynomial function vectors; $\mathbf{u}$, $\mathbf{v}$ and $\mathbf{w}$ are vectors containing the generalized coordinate variables.

Substituting Eqs. (2)-(6) into Eq. (1) and omitting the harmonic time dependence $e^{i\omega t}$, the discretized equations of motion of the coupled shell can be described as follows

$$-\omega^2\mathbf{M}_s\tilde{\mathbf{q}} + \left(\mathbf{K}_s - \mathbf{K}_\lambda + \mathbf{K}_\kappa\right)\tilde{\mathbf{q}} = \mathbf{f}_s + \mathbf{f}_{\text{p}} \tag{7}$$

$\tilde{\mathbf{q}}$ is the vector of global generalized coordinates. $\mathbf{M}_s$ and $\mathbf{K}_s$ are respectively the disjoint generalized mass and stiffness matrices of the coupled shell, which are obtained by the assembly of the corresponding segment matrices. $\mathbf{K}_\lambda$ and $\mathbf{K}_\kappa$ are the generalized interface stiffness matrices generated by the interface potentials. $\mathbf{f}_s$ is the generalized force vector due to external structural excitation. $\mathbf{f}_\mathrm{p}$ is the generalized load vector representing the acoustic fluid pressure acting on the shell. Dissipation within the coupled shell is introduced in the form of a complex Young's modulus $E = E(1+i\eta)$, where η is the loss factor associated with internal dissipation.

The sound pressure p radiated by the coupled shell satisfies the Kirchhoff-Helmholtz integral equation (2)

$$C(\mathbf{r})\,p(\mathbf{r}) = \int_{S_0}\left[\, p(\mathbf{r}_0)\frac{\partial G(\mathbf{r},\mathbf{r}_0)}{\partial \bar{n}} - G(\mathbf{r},\mathbf{r}_0)\frac{\partial p(\mathbf{r}_0)}{\partial \bar{n}}\right] dS \tag{8}$$

where $\mathbf{r}(r,\theta,z)$ and $\mathbf{r}_0(r_0,\theta_0,z_0)$ are respectively the field point vectors exterior to and on the exterior acoustic surface S_0. The quantity $C(\mathbf{r})$ is a coefficient depending on the position of field point $\mathbf{r}$, given as follows: $C(\mathbf{r})=1$ for $\mathbf{r}$ inside the acoustic domain, $C(\mathbf{r})=0$ for $\mathbf{r}$ outside the acoustic domain, and $C(\mathbf{r})=0.5$ for $\mathbf{r}$ on the acoustic surface S_0. $\bar{n}$ is the outward normal direction at a point on the shell surface. $\partial/\partial\bar{n}$ denotes the outward normal derivative. $G(\mathbf{r},\mathbf{r}_0)$ is the three-dimensional free-space Green's function, expressed as:

$$G(\mathbf{r},\mathbf{r}_0) = \frac{e^{-ikR_0}}{4\pi R_0} \tag{9}$$

where k is the acoustic wave number. R_0 is the geometrical distance between points $\mathbf{r}$ and $\mathbf{r}_0$ defined as $R_0(\mathbf{r},\mathbf{r}_0) = |\mathbf{r}-\mathbf{r}_0|$.

Considering the axisymmetric property of the coupled shell, the variables $p(\mathbf{r})$, $p(\mathbf{r}_0)$, $G(\mathbf{r},\mathbf{r}_0)$ and $\partial G(\mathbf{r},\mathbf{r}_0)/\partial\bar{n}$ in Eq. (8) can be expanded by a Fourier series as follows:

$$p(\mathbf{r}) = \sum_{n=0}^{\tilde{N}}\left[\, p_n^{\mathrm{sy}}(r,n,z)\sin(n\theta) + p_n^{\mathrm{nsy}}(r,n,z)\cos(n\theta)\right] \tag{10a}$$

$$p(\mathbf{r}_0) = \sum_{n=0}^{\tilde{N}}\left[\, \bar{p}_n^{\mathrm{sy}}(r_0,n,z_0)\sin(n\theta_0) + \bar{p}_n^{\mathrm{nsy}}(r_0,n,z_0)\cos(n\theta_0)\right] \tag{10b}$$

$$G(\mathbf{r},\mathbf{r}_0) = \frac{1}{\pi}\sum_{n=0}^{\tilde{N}} H_n\left[\sin(n\theta)\sin(n\theta_0) + \cos(n\theta)\cos(n\theta_0)\right] \tag{10c}$$

$$\frac{\partial G(\mathbf{r},\mathbf{r}_a)}{\partial\bar{n}} = \sum_{n=0}^{\tilde{N}}\frac{1}{\pi}\bar{H}_n\left[\sin(n\theta)\sin(n\theta_0) + \cos(n\theta)\cos(n\theta_0)\right] \tag{10d}$$

p_n^{sy} and p_n^{nsy} are Fourier coefficients of $p(\mathbf{r})$. $\bar{p}_n^{\mathrm{sy}}$ and $\bar{p}_n^{\mathrm{nsy}}$ are Fourier coefficients of $p(\mathbf{r}_0)$. H_n and $\bar{H}_n$ are Fourier coefficients of the Green's function and its normal derivative, which can be determined by standard Fourier transformation as follows

$$H_n = \int_0^{2\pi}\frac{e^{-ikR_0}}{4\pi R_0}\cos(n\theta)\,d\theta, \qquad \bar{H}_n = \int_0^{2\pi}\frac{\partial}{\partial\bar{n}}\left(\frac{e^{-ikR_0}}{4\pi R_0}\right)\cos(n\theta)\,d\theta \tag{11}$$

The surface pressure $p(\mathbf{r}_0)$ can be related to the normal displacement component w of the coupled shell by

$$\frac{\partial p(\mathbf{r}_0)}{\partial\bar{n}} = \rho_f\omega^2 w \tag{12}$$

where ρ_f is the density of the fluid.

Substituting Eq. (10) into Eq. (8) and using the orthogonality properties for integrals involving trigonometric series, a modified form of the Kirchhoff-Helmholtz integral equation is obtained as follows:

$$C(\mathbf{r})\,p_n^{\mathrm{sy}} = \int_l\left(\bar{H}_n\bar{p}_n^{\mathrm{sy}} - \rho_f\omega^2 H_n\tilde{w}_n^{\mathrm{sy}}\right)r_0\,dl, \quad C(\mathbf{r})\,p_n^{\mathrm{nsy}} = \int_l\left(\bar{H}_n\bar{p}_n^{\mathrm{nsy}} - \rho_f\omega^2 H_n\tilde{w}_n^{\mathrm{nsy}}\right)r_0\,dl \tag{13}$$

For the m^{th} shell segment, the Fourier coefficients of the pressure corresponding to $\bar{p}_n^s$ and $\bar{p}_n^c$ are expanded by orthogonal polynomials as follows

$$\bar{p}_n^{m,\upsilon} = \sum_{j=0}^{J-1} P_j^{\upsilon}(\xi)\bar{p}_j^{m,\upsilon} = \bar{\mathbf{P}}_n^{m,\upsilon}\bar{\mathbf{p}}_n^{m,\upsilon} \quad ,\upsilon = \text{sy, nsy} \tag{14}$$

$P_j^{\upsilon}(\xi)$ is the j^{th} order Chebyshev orthogonal polynomials of the first kind. J is the highest degree taken in the Chebyshev polynomials. ξ is a dimensionless local coordinate varying in [-1,1]. $\bar{\mathbf{P}}_n^{m,\upsilon}$ is the polynomial function vector. $\bar{\mathbf{p}}_n^{m,\upsilon}$ is the column vector containing generalized pressure variables.

Substituting Eq. (14) into Eq. (13), the two Helmholtz integrals can be combined and written in a compact form as

$$C\bar{\mathbf{P}}_n(\mathbf{r}_i)\bar{\mathbf{p}}_n(\mathbf{r}_i) = \sum_{m=1}^{N}\left(\int_{l_m} \bar{H}_n\bar{\mathbf{P}}_n^m r_0 dl_m\right)\bar{\mathbf{p}}_n^m - \sum_{m=1}^{N}\left(\int_{l_m} \rho_f\omega^2 H_n\mathbf{W}_n^m r_0 dl_m\right)\tilde{\mathbf{w}}_n^m \tag{15}$$

For the solution process, a collocation scheme is applied to the above equation. The collocation points $\mathbf{r}_i(\xi)$ are naturally taken as the roots of the Chebyshev polynomial of the first kind. In the local coordinate, the roots ξ_j are given as: $\xi_j = \cos[(2j-1)\pi/(2J)]$, $j = 1,2,\cdots,J$. This collocation method results in a set of $(N_c + 2N_s)\times J$ linear algebraic equations for each circumferential mode number. Considering circumferential mode numbers $n = 0,1,\cdots,\tilde{N}$, the following equation is obtained:

$$\bar{\mathbf{H}}\bar{\mathbf{p}} = \mathbf{G}\tilde{\mathbf{w}} \tag{16}$$

where $\bar{\mathbf{H}}$ and $\mathbf{G}$ are coefficient matrices for all circumferential mode numbers, expressed as $\bar{\mathbf{H}} = \text{diag}[\bar{\mathbf{H}}_0, \bar{\mathbf{H}}_1, \cdots, \bar{\mathbf{H}}_n, \cdots, \bar{\mathbf{H}}_{\tilde{N}}]$ and $\mathbf{G} = \text{diag}[\mathbf{G}_0, \mathbf{G}_1, \cdots, \mathbf{G}_n, \cdots, \mathbf{G}_{\tilde{N}}]$. $\bar{\mathbf{H}}_n$ and $\mathbf{G}_n$ are the coefficient matrices related to circumferential mode number n. $\bar{\mathbf{p}}$ and $\tilde{\mathbf{w}}$ are the vectors containing the generalized pressure variables and the normal displacement components of the shell, respectively.

Inserting Eqs. (6), (10) and (14) into Eq. (5), and introducing the coordinate transformation: $\tilde{\mathbf{w}} = \mathbf{T}\tilde{\mathbf{q}}$, the generalized load vector $\mathbf{f}_{\text{p}}$ in Eq. (7) is obtained as:

$$\mathbf{f}_{\text{p}} = -\mathbf{T}^{\text{T}}\bar{\mathbf{G}}\tilde{\mathbf{H}}^{-1}\mathbf{G}\mathbf{T}\tilde{\mathbf{q}} = -\left[-\omega^2\mathbf{M}_{\text{f}}(\omega) + i\mathbf{C}_{\text{f}}(\omega)\right]\tilde{\mathbf{q}} \tag{17}$$

where $\bar{\mathbf{G}}$ is the fluid-structure coupling matrix, defined as $\bar{\mathbf{G}} = \text{diag}[\tilde{\mathbf{G}}_1, \tilde{\mathbf{G}}_2, \cdots, \tilde{\mathbf{G}}_n, \cdots, \tilde{\mathbf{G}}_{\tilde{N}}]$. $\tilde{\mathbf{G}}_n$ is the coupling matrix for circumferential mode n given by $\tilde{\mathbf{G}} = \text{diag}[\hat{\mathbf{G}}_1, \hat{\mathbf{G}}_2, \cdots, \hat{\mathbf{G}}_m, \cdots, \hat{\mathbf{G}}_N]$, in which $\hat{\mathbf{G}}_m = \iint_{S_m} \mathbf{W}^{m,\text{T}}\bar{\mathbf{P}}^m dS$. $-\omega^2\mathbf{M}_{\text{f}}$ and $\mathbf{C}_{\text{f}}$ are frequency-dependent matrices, which are the real and imaginary parts of $\mathbf{T}^{\text{T}}\bar{\mathbf{G}}\tilde{\mathbf{H}}^{-1}\mathbf{G}\mathbf{T}$, respectively.

Substituting Eq. (17) into Eq. (7), the governing equation for the fluid-structure interaction problem of the coupled shell becomes

$$-\omega^2\left[\mathbf{M}_s + \mathbf{M}_{\text{f}}(\omega)\right]\tilde{\mathbf{q}} + i\mathbf{C}_{\text{f}}(\omega)\tilde{\mathbf{q}} + \left(\mathbf{K}_s - \mathbf{K}_\lambda + \mathbf{K}_\kappa\right)\tilde{\mathbf{q}} = \mathbf{f}_{\text{s}} \tag{18}$$

The above equation indicates that the effect of the fluid can be viewed as added mass and damping. Once $\tilde{\mathbf{q}}$ is known, the generalized pressure vector $\bar{\mathbf{p}}$ on the acoustic boundary is computed accordingly by Eq. (16). Then, the pressure at any position in the fluid can be determined from Eqs. (10) and (15).

2.3 Numerical Model

A numerical model using finite elements for the structure and boundary elements to represent the exterior fluid is developed to predict the acoustic responses of the fully coupled problem. The coupling conditions at the fluid-structure interface corresponding to equilibrium of the acoustic pressure and the normal stress at the interface and the continuity of the velocities of the fluid particles and the structure in the normal direction across the interface. This leads to a global system of equations as follows (10)

$$\begin{bmatrix} \mathbf{K} - \omega^2\mathbf{M} & -\mathbf{C}_{sf} \\ -i\omega\mathbf{G}\mathbf{C}_{fs} & \mathbf{H} \end{bmatrix}\begin{bmatrix} \mathbf{u} \\ \mathbf{p} \end{bmatrix} = \begin{bmatrix} \mathbf{f}_s \\ \mathbf{p}_i \end{bmatrix} \tag{19}$$

The matrices **K** and **M** are the stiffness and mass matrices of the structure, respectively and are constructed using the software package ANSYS. The matrices **H** and **G** are the BEM influence matrices obtained through collocation using AKUSTA (11). The vectors **p** and **u** are, respectively, the vectors with the nodal values for pressure and displacement. The vectors $\mathbf{f}_s$ and $\mathbf{p}_i$ are the nodal structural forces and the nodal values of the incident pressure field, respectively. ω is the angular frequency and i is the imaginary unit. $\mathbf{C}_{sf}$ and $\mathbf{C}_{fs}$ are structural-acoustic coupling matrices. The radiated sound power P is defined as

$$P = \frac{1}{2}\Re\left\{\mathbf{v}_f^{\mathrm{T}}\mathbf{Z}\mathbf{v}_f^{*}\right\} \tag{20}$$

where $\mathbf{v}_f$ is the particle velocity and **Z** is the acoustic impedance matrix. The contributions of the fluid-loaded structural modes to the radiated sound power are given by (8)

$$P_{ij} = \frac{1}{2}\omega^2\mathbf{d}_i^{\mathrm{T}}\mathbf{Z}\mathbf{d}_j^{*} \tag{21}$$

where $\mathbf{d}_i$ is the modal fluid displacement vector.

3. RESULTS AND DISCUSSION

Results for the sound pressure and power radiated by the coupled shell under different external loads are compared using the semi-analytical and numerical methods. The geometrical dimensions of the cylindrical shell are length $L = 45\,\mathrm{m}$, radius $R = 3.25\,\mathrm{m}$ and thickness $h = 0.04\,\mathrm{m}$. The two hemispherical end caps also have $R = 3.25\,\mathrm{m}$ and $h = 0.04\,\mathrm{m}$. The overall length of the coupled structure is 51.5m. The coupled shell structure is made from steel with material data given as Young's modulus $E = 210\,\mathrm{GPa}$, Poisson's ratio $\mu = 0.3$ and density $\rho = 7860\,\mathrm{kg/m^3}$. The coupled shell is submerged in either air or water. For air, the density and speed of sound are respectively given as $\rho_f = 1.204\,\mathrm{kg/m^3}$ and $c_f = 340\,\mathrm{m/s}$, and $\rho_f = 1000\,\mathrm{kg/m^3}$, $c_f = 1482\,\mathrm{m/s}$ are considered for water. Three types of excitation loads are examined corresponding to an axial point force, and axial and transverse ring forces, as shown in Figure 2. The point force is acting in the axial direction at the junction of the cylindrical shell and hemispherical shell at the left end, of which the location defined in the global cylindrical coordinate system is given as $(r,\ \theta,\ z) = (R,\ 0,\ -L/2)$. The ring force in the axial or transverse direction is applied uniformly at the junction of the cylindrical shell and hemispherical shell at the left end. The magnitude of each force is unity. In the global cylindrical coordinate system, the transverse ring force can be decomposed into the following relations: $f_u = 0$, $f_v = \cos\theta/(2\pi R)$, $f_w = \sin\theta/(2\pi R)$.

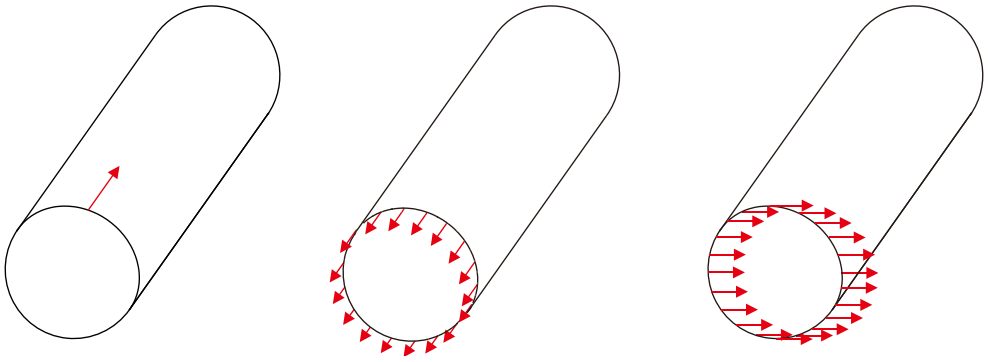

Figure 2 – Loading cases for the cylindrical shell with hemispherical end caps

Figure 3 presents the radiated sound power of the coupled shell subject to the axial ring force. The surrounding acoustic medium is air. Structural damping of the coupled shell was not considered, that is, $\eta = 0$. In the semi-analytical model, the cylindrical shell was discretized into N_c =14 segments and each hemispherical end cap was divided into N_s =4 segments. For each segment, the terms of the Chebyshev orthogonal polynomials expanded are $Q = 7$ for the displacement components and $J = 2$ for the sound pressure. Since the axial ring force can only excite axisymmetric vibration modes of the coupled shell, the circumferential mode number of the

displacement and pressure variables is truncated as $\bar{N} = \tilde{N} = 0$. In the fully coupled numerical FE/BE model, the structure is discretized using quadratic finite shell elements (Shell281 in ANSYS 12.1), and the fluid of infinite extent is modelled using super-parametric discontinuous linear boundary elements. The two models are coupled using a mortar coupling method adapted for quadratic shape functions (10). As shown in Figure 3, a comparison of the results for the sound power obtained semi-analytically and numerically is found to be excellent. Under axial ring excitation, the peaks in the radiated sound power correspond to successive $n = 0$ circumferential modes of the shell.

Figure 4 presents the radiated sound power for the coupled cylindrical/hemispherical shell subject to transverse ring force excitation. Again, the external fluid is assumed to be air and the structural loss factor of the shell is taken as $\eta = 0$. For the shell subject to the transverse ring force, only the rigid and elastic modes corresponding to successive $n = 1$ modes are excited. In the semi-analytical model, the circumferential mode number of the displacement and pressure variables is chosen as $\bar{N} = \tilde{N} = 1$. Similar to Figure 3, excellent agreement in the results for the radiated sound power obtained from the semi-analytical model and the fully coupled FE/BE model can be observed. Under the transverse ring excitation, the peaks in the radiated power correspond to successive $n = 1$ bending modes of the coupled shell.

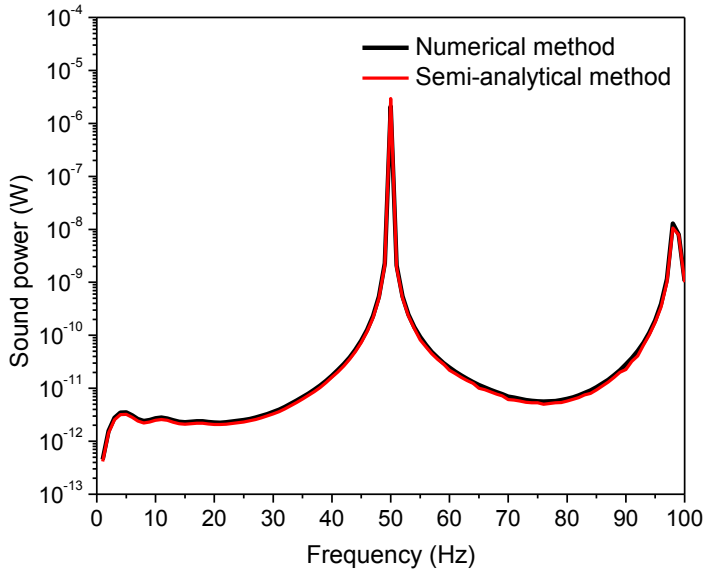

Figure 3 – Sound power of the coupled shell immersed in air and under axial ring force excitation

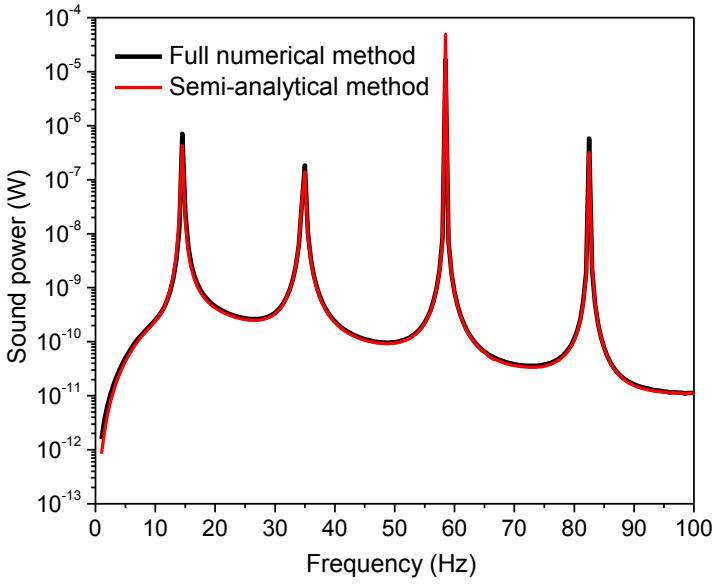

Figure 4 – Sound power of the coupled shell immersed in air and under transverse ring force excitation

Figure 5 shows the radiated sound power of the coupled shell immersed in water and subject to an axial point force at the junction of the cylindrical and hemispherical shells at one end. The point force excitation represents a more complex excitation case than ring force excitation as it excites all axisymmetric and non-axisymmetric vibration modes of the shell. Structural damping is considered with the loss factor taken as $\eta = 0.01$ in both the semi-analytical and numerical models. As for the previous results, in the semi-analytical model the cylindrical shell was discretized with $N_c = 14$ segments and the hemispherical shells were discretized with $N_s = 4$ segments each. This excitation case results in excitation of the $n = 0$ breathing and $n = 1$ bending modes, as well as excitation of higher order circumferential models of the coupled shell. It is observed in Figure 5 that the results for the radiated sound power obtained from the semi-analytical model agree well with those from the fully coupled FE/BE model.

In Figure 6, the modal contributions from individual circumferential modes to the radiated sound power of the coupled shell are presented. Again, the shell is submerged in water and under axial point force excitation. Structural damping is assumed as $\eta = 0$. Contributions to the radiated sound power for grouped $n = 0$, grouped $n = 1$ and grouped $n = 2:10$ circumferential modes. It is observed from Figure 6 that the higher order circumferential modes ($n \geq 2$) do not significantly contribute to the radiated sound power for the frequency range considered. This implies that even though the vibration modes corresponding to higher circumferential mode numbers of the coupled shell may be excited by the point force, only successive $n = 0$ axisymmetric breathing modes and successive $n = 1$ bending modes contribute to the overall sound radiation.

Figure 7 presents the directivity patterns for the first two resonances of the coupled shell immersed in water and excited by an axial point force, corresponding to 40 Hz and 54 Hz as shown in Figure 5. The directivity pattern is plotted at a distance of $R_P = 1000\,\text{m}$ with $0 \leq \phi \leq 360^0$, where R_P and ϕ are defined in Figure 1. In Figures 7(a) and 7(b), the total radiated sound pressure and modal contributions grouped by the $n = 0$, $n = 1$ and $n = 2:10$ circumferential modes of the coupled shell are presented. As expected, for the two frequencies considered, the $n = 2:10$ modes do not significantly contribute to the far-field radiated sound pressure. In Figure 7(a), the $n = 0$ breathing modes dominate the total far-field sound pressure since the chosen frequency of 40 Hz corresponds to an $n = 0$ resonance. In Figure 7(b), both the $n = 0$ breathing modes and $n = 1$ bending modes contribute to the total far-field sound pressure. However, the contribution to the total sound pressure is greater from the $n = 1$ modes than from the $n = 0$ modes since the chosen frequency of 54 Hz corresponds to an $n = 1$ bending resonance. By observing the individual contributions of the circumferential modes to the sound power and directivity of the radiated sound pressure, greater physical insight into the fluid-structure interaction problem of the coupled cylindrical shell can be obtained.

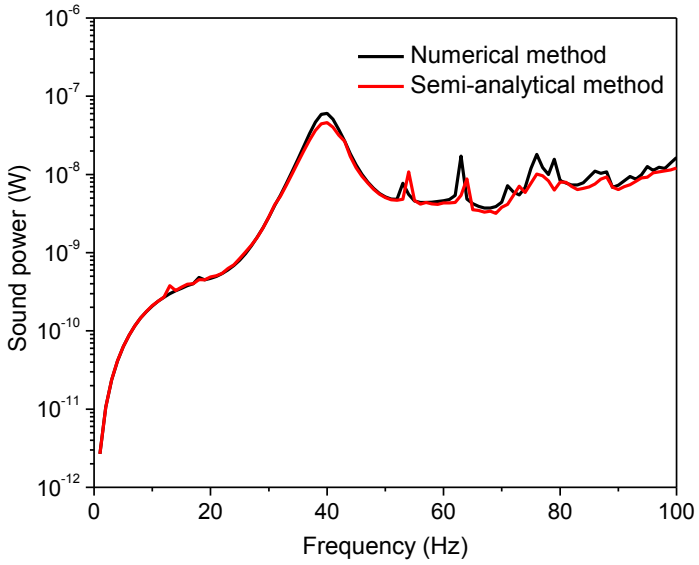

Figure 5 – Radiated sound power of the coupled shell in water and under axial point force excitation

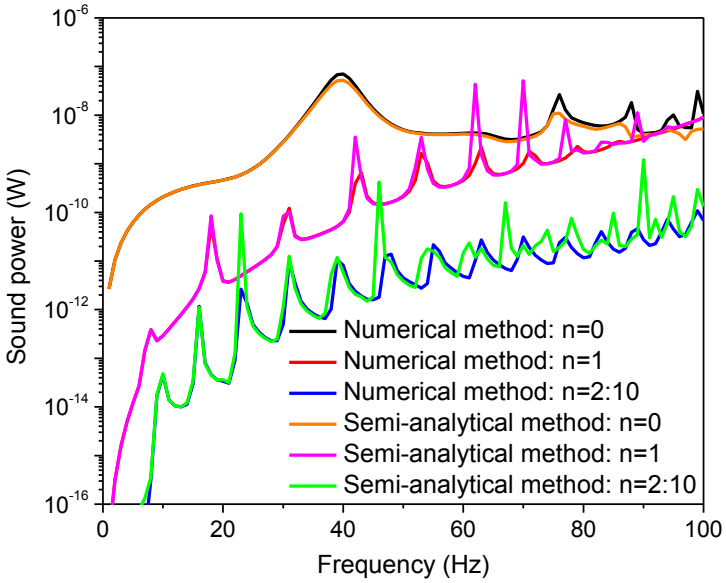

Figure 6 - Modal contributions from grouped circumferential modes to the radiated sound power of the coupled shell in water and under axial point force excitation

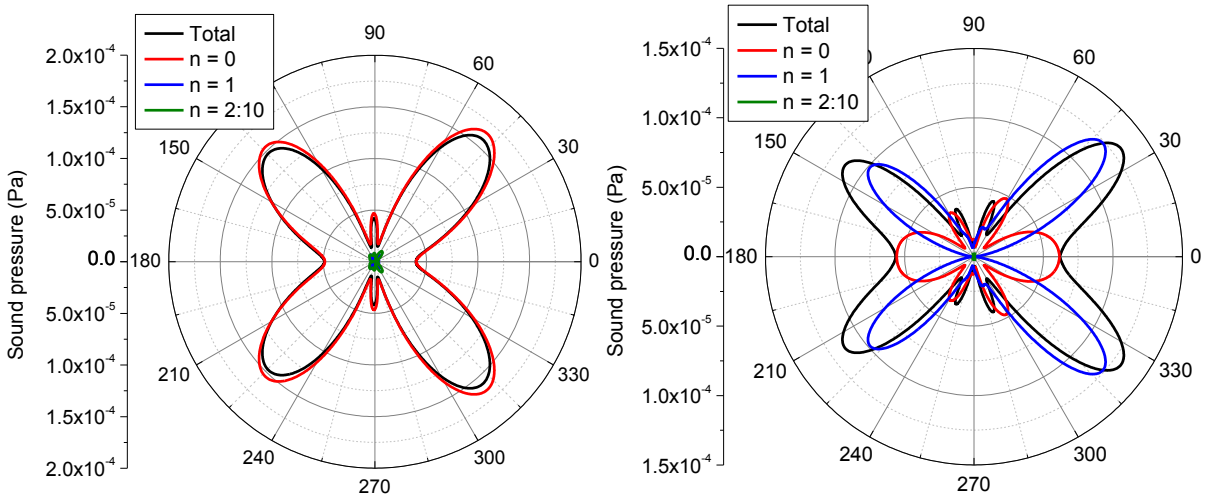

(a) (b)

Figure 7 - Directivity plots for the shell immersed in water and under axial point force: (a) 40Hz; (b) 54Hz

4. CONCLUSIONS

Modal contributions to the radiated sound power and far-field sound pressure for a cylindrical shell with two hemispherical end caps submerged in a fluid medium are investigated using both semi-analytical and numerical methods. For the semi-analytical method, the Reissner's thin shell theory combined with a modified variational method is employed to formulate the structural model of the shell, whereas a spectral boundary element method is used to model the external fluid loading. The displacement and sound pressure variables are expanded by Fourier series and Chebyshev orthogonal polynomials. As a result, a two-dimensional problem is transformed into a set of uncoupled one-dimensional problems, which correspond to the harmonics of the Fourier expansion. Numerical solutions obtained using a fully coupled finite element/boundary element model are also presented. The modal contributions to the radiated sound power and far-field sound pressure for the coupled shell immersed in air/water and subjected to different excitation forces are investigated. Identifying the individual contributions of circumferential modes to the radiated sound power and directivity of the radiated sound pressure provides greater physical insight into the structure-borne noise characteristics of fluid-loaded shells.

REFERENCES

1. Junger MC, Feit D. Sound, Structures, and Their Interaction, 2nd ed. Cambridge, USA: MIT Press; 1986.
2. Fahy F, Gardonio P. Sound and Structural Vibration Radiation, Transmission and Response, 2nd ed. Oxford, UK: Academic Press; 2007.
3. Skelton EA, James JH. Theoretical Acoustics of Underwater Structures. London, UK: Imperial College Press; 1997.
4. Wilton DT. Acoustic radiation and scattering from elastic structures. Int J Numer Meth Eng. 1978; 13(1):123-138.
5. Jeans RA, Mathews IC. Solution of fluid-structure interaction problems using a coupled finite element and variational boundary element technique. J Acoust Soc Am. 1990; 88(5): 2459-2466.
6. Merz S, Oberst S, Dylejko PG, Kessissoglou NJ, Tso YK, Marburg S. Development of coupled FE/BE models to investigate the structural and acoustic responses of a submerged vessel. J Comp Acoust. 2007; 15(1): 23-47.
7. Merz S, Kinns R, Kessissoglou NJ. Structural and acoustic responses of a submarine hull due to propeller forces. J Sound Vib. 2009; 325:266-286.
8. Peters H, Kessissoglou N, Marburg S. Modal decomposition of exterior acoustic-structure interaction problems with model order reduction. J Acoust Soc Am. 2014; 135(5): 2706-2717.
9. Qu Y, Wu S, Chen Y, Hua H. Vibration analysis of ring-stiffened conical-cylindrical-spherical shells based on a modified variational approach. Int J Mech Sci. 2013; 69:72-84.
10. Peters H, Marburg S, Kessissoglou N. Structural-acoustic coupling on non-conforming meshes with quadratic shape functions. Int J Num Meth Eng. 2012; 91:27-38.
11. Marburg S, Schneider S. Influence of element types on numeric error for acoustic boundary elements. J Comp Acoust. 2003; 11(3): 363-386.